Kinetics of Two Pathways in Peroxyoxalate Chemiluminescence

Andrew G. Hadd, Anke Seeber, and John W. Birks*

Department of Chemistry and Biochemistry and Cooperative Institute for Research in Environmental Sciences (CIRES), University of Colorado, Boulder, Colorado, 80309

Received November 9, 1999

It has been shown that 1,1′-oxalyldiimidazole (ODI) is formed as an intermediate in the imidazole-catalyzed reaction of oxalate esters with hydrogen peroxide. Therefore, the kinetics of the chemiluminescence reaction of 1,1′-oxalyldiimidazole (ODI) with hydrogen peroxide in the presence of a fluorophore was investigated in order to further elucidate the mechanism of the peroxyoxalate chemiluminescence reaction. The effects of concentrations of ODI, hydrogen peroxide, imidazole (ImH), the general-base catalysts lutidine and collidine, and temperature on the chemiluminescence profile and relative quantum efficiency in the solvent acetonitrile were determined using the stopped-flow technique. Pseudo-first-order rate constant measurements were made for concentrations of either H_2O_2 or ODI in large excess. All of the reaction kinetics are consistent with a mechanism in which the reaction is initiated by a base-catalyzed substitution of hydrogen peroxide for imidazole in ODI to form an imidazoyl peracid ($Im(CO)_2OOH$). In the presence of a large excess of H_2O_2, this intermediate rapidly decays with both a zero- and first-order dependence on the H_2O_2 concentration. It is proposed that the zero-order process reflects a cyclization of this intermediate to form a species capable of exciting a fluorophore via the "chemically initiated electron exchange mechanism" (CIEEL), while the first-order process results from the substitution of an additional molecule of hydrogen peroxide to the imidazoyl peracid to form dihydroperoxyoxalate, reducing the observed quantum yield. Under conditions of a large excess of ODI, the reaction is more than 1 order of magnitude more efficient at producing light, and the quantum yield increases linearly with increasing ODI concentration. Again, it is proposed that the slow initiating step of the reaction involves the substitution of H_2O_2 for imidazole to form the imidazoyl peracid. This intermediate may decay by either cyclization or by reaction with another ODI molecule to form a cyclic peroxide that is much more efficient at energy transfer with the fluorophore. The reaction kinetics clearly distinguishes two separate pathways for the chemiluminescent reaction.

Introduction

The peroxyoxalate chemiluminescence (PO-CL) reaction has become widely used for analytical detection schemes based on chemiluminescence.[1] However, the details of the reaction mechanism, including the number and nature of the reactive intermediates that lead to chemiluminescence is still not fully understood.[2−6] We are interested in understanding the mechanism of the PO-CL reaction in order to improve its analytical sensitivity. This paper is the third in a sequence of articles that that seeks to elucidate and quantify the PO-CL reaction mechanism.[7,8]

Imidazole has been widely used as a catalyst for the PO-CL reaction, and in comparison with other amine bases, imidazole has the greatest effect on the chemiluminescence yield and kinetics.[9] The complex effect of imidazole on the reaction kinetics has been attributed to a combination of "nucleophilic" and "general-base" catalysis.[4] Nucleophilic catalysis with intermediate formation of an acyl-imidazole has been observed in imidazole-catalyzed hydrolysis reactions.[10−12] Since 1,1′-oxalyldiimidazole (ODI) has been observed in the nucleophilic reaction of imidazole with aryl oxalate esters[7,12] and shown to be a key intermediate in the imidazole-catalyzed PO-CL reaction,[6,8,13] we have analyzed the kinetics of the imidazole-catalyzed reaction of ODI with hydrogen peroxide.

The effects of each of the reagents on the chemiluminescence yields and reaction kinetics were determined under pseudo-first-order conditions with either ODI or hydrogen peroxide in large excess. The reaction was studied with and without catalysis by imidazole or the general base catalysts lutidine and collidine in order to clarify the role of imidazole in the formation and destruction of reactive intermediates. The temperature dependencies of the pseudo-first-order rate constants also were

* To whom correspondence should be addressed.

(1) (a) Robards, K.; Worsfold, P. J. *Anal. Chim. Acta* **1992**, *266*, 147−173. (b) Hadd, A. G.; Birks, J. W. In *Peroxyoxalate Chemiluminescence: Mechanism and Analytical Detection*; Sievers, R. E., Ed.; John Wiley and Sons: New York, NY, 1995; pp 209−239.

(2) Rauhut, M. M.; Bollyky, L. J.; Roberts, B. G.; Loy, M.; Whitman, R. H.; Iannotta, A. V.; Semsel, A. M.; Clake, R. A. *J. Am. Chem. Soc.* **1967**, *89*, 9, 6515−6522.

(3) Catherall, C. L.; Palmer, T. F.; Cundall, R. B. *J. Chem. Soc., Faraday Trans. 2* **1984**, *80*, 837−849.

(4) Orlovic, M.; Schowen, R. L.; Givens, R. S.; Alvarez, F.; Matusweski, B.; Parekh, N. *J. Org. Chem.* **1989**, *54*, 3605.

(5) Milofsky, R. E.; Birks, J. W. *J. Am. Chem. Soc.* **1991**, *113*, 9715−9723.

(6) Stevani, C. V.; Lima, D. F.; Toscano, V. G.; Baader, W. J. *J. Chem. Soc., Perkin Trans. 2* **1996**, 989.

(7) Hadd, A. G.; Birks, J. W. *J. Org. Chem.* **1996**, *61*, 2657−2663.

(8) Hadd, A. G.; Robinson, A. L.; Rowlen, K. L.; Birks, J. W. *J. Org. Chem.* **1998**, *63*, 3023−3031.

(9) Hanaoka, N.; Givens, R. S.; Schowen, R. L.; Kuwana, T. *Anal. Chem.* **1988**, *60*, 2193-2197.

(10) Bender, M. L.; Turnquest, B. W. *J. Am. Chem. Soc.* **1957**, *79*, 1652.

(11) Kirsch, J. F.; Jencks, W. P. *J. Am. Chem. Soc.* **1964**, *86*, 833−846.

(12) Neuvonen, H. *J. Chem. Soc., Perkin Trans. 2* **1990**, 669.

(13) Stigbrand, M.; Ponten, E.; Irgum, K. *Anal. Chem.* **1994**, *66*, 1766.

10.1021/jo9917487 CCC: $19.00
Published on Web 04/12/2000

determined in order to provide additional clues to the complex reaction mechanism. An important finding is that the reaction proceeds along very different pathways depending on which reagent, H_2O_2 or ODI, is in large excess.

Experimental Section

Chemicals. Imidazole (ImH), 9,10-diphenylanthracene (DPA), and 1,1′-oxalyldiimidazole (ODI, 90% technical grade) were obtained from Aldrich. Hydrogen peroxide (H_2O_2), 30% solution in water, was purchased from Fischer. The concentration of H_2O_2 was determined by titration with a standardized thiosulfate solution prior to dilution. Acetonitrile, Burdick and Jackson HPLC grade, was used for all experiments. Stock solutions of ODI, 1.0 mM, were prepared by dissolving 9.5 mg in 50.0 mL of acetonitrile. Fresh solutions were prepared every 4 h and stored in the dark.

Chemiluminescence Measurements. An Applied Photophysics DX-17MV stopped-flow spectrophotometer (Leatherhead, UK) was used for all chemiluminescence measurements. The instrument was operated with the lamp turned off and was thermostated using a Neslab RTE-11 circulating cooler. In a typical experiment, a stock solution of 0.20 mM ODI and 0.20 mM DPA was prepared and added to one syringe of the stopped-flow instrument. Mixtures of hydrogen peroxide, 5.0−40.0 mM, with and without imidazole, 10.0 mM, were used in the other syringe. Chemiluminescence profiles of signal versus time were acquired as a function of the concentration of each of the reagents, ODI, imidazole, and H_2O_2. Tabulated reagent concentrations reflect the final post-mixing concentration. Unless otherwise noted, 0.10 mM DPA was used for all chemiluminescence measurements. The profile area, which is proportional to the chemiluminescence quantum yield, was obtained by integrating the signal-versus-time plots and is reported in arbitrary units (au). Unless otherwise stated, measured rate constants refer to an ambient temperature of 25 °C.

Kinetics Measurements Based on Absorbance. Additional kinetics information was obtained using the stopped-flow spectrophotometer by studying the change in absorbance of ODI at 245 nm upon reaction with an excess of H_2O_2 in the absence of a fluorophore.

Analysis of Rate Data. A simplified model for evaluating the kinetics of the chemiluminescence reaction has been developed[4,5]

$$\mathrm{A} \xrightarrow{k'_1} \mathrm{B} \xrightarrow{k'_2} \mathrm{C} \qquad (1)$$

where **A**, **B**, and **C** represent pools of reactants, intermediates, and products, respectively, and both reaction steps are irreversible first-order reactions. The chemiluminescence signal is proportional to the concentration of intermediate(s) **B**, and the integrated rate equation for the chemiluminescence intensity versus time is

$$I = \frac{Mk'_1}{k'_1 - k'_2}(e^{-k'_2 t} - e^{-k'_1 t}) \qquad (2)$$

Using this simplified scheme, the two pseudo-first-order rate constants, k'_1 and k'_2, were obtained for all chemiluminescence signal-versus-time profiles from a nonlinear least-squares fit to eq 2. An example of profiles obtained is shown in Figure 1 for the imidazole-catalyzed reaction of 0.10 mM ODI with various excess H_2O_2 concentrations in the presence of 5 mM imidazole.

Note that since the shape of the intensity profile given in eq 2 is symmetric with respect to exchanging the two rate constants, k'_1 and k'_2, there are two equally good solutions to a least-squares fit. These two possible solutions reveal an ambiguity in evaluating rise-fall kinetics data using only the temporal changes in **B**. We originally evaluated our data by ascribing the faster process to k'_1, which visually reflects the rise in the chemiluminescence signal (see Figure 1). However, as described below, a stopped-flow study with UV absorption to follow the loss of ODI in a large excess of H_2O_2 proved that the slower "fall" reaction actually describes the process **A** → **B** with rate constant k'_1 and the faster "rise" reaction describes the process **B** → **C** with rate constant k'_2.

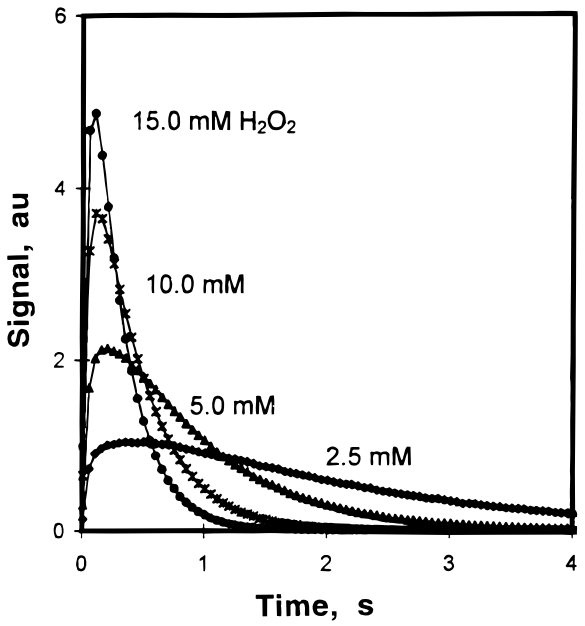

Figure 1. Chemiluminescence intensity versus time profiles obtained as a function of hydrogen peroxide concentration using imidazole catalysis. Conditions: 0.10 mM ODI, 5.0 mM imidazole, and 0.10 mM DPA.

Results and Discussion

Measurement of the Rate of Reaction of ODI with Excess H_2O_2 by UV Absorption in the Absence of a Fluorophore. The decrease in UV absorbance of ODI was followed at 245 nm (where it absorbs much more strongly than ImH) in the reaction of 0.10 mM ODI with 2.0 mM H_2O_2 for imidazole ranging in concentration from 2.5 to 10.0 mM. For these experiments, no fluorophore was present. The change in absorbance with time was well described by a single-exponential decay with first-order rate constants of 0.25, 0.49, 0.70, and 0.95 s^{-1} for 2.5, 5.0, 7.5, and 10.0 mM ImH, respectively. By comparison, the chemiluminescence signal obtained for identical reaction conditions, but adding 0.10 mM DPA as a fluorophore, is described by a fast rise time (>20 s^{-1}) followed by exponential decay with rate constants of 0.22, 0.50, 0.73, and 0.92 s^{-1} for the same series of ImH concentrations. This excellent agreement indicates that the slow component of the chemiluminescence profile (the "fall" component) corresponds to the loss of ODI. Assuming that the first step of the reaction involves transformation of ODI to a less strongly absorbing compound (e.g., nucleophilic substitution of ImH with H_2O_2), the decrease in the ODI absorbance reflects the reaction process A → B, and therefore the slow decay of the chemiluminescence signal, as in Figure 1, represents k'_1, the formation of intermediates from ODI.

Effect of Temperature and Hydrogen Peroxide Concentration on the Imidazole-Catalyzed Reaction of ODI with an Excess of H_2O_2. The chemiluminescence signal-versus-time profiles for H_2O_2 concentra-

Table 1. Variation of k'_1 and k'_2 with H_2O_2 Concentation as a Function of Temperature in the Imidazole-Catalyzed Reaction of ODI with an Excess of H_2O_2[a]

$[H_2O_2]$, mM	7.1 °C	15.1 °C	24.9 °C	35.3 °C	45.1 °C
		k'_1, s^{-1}			
2.50	0.545 ± 0.003	0.45 ± 0.01	0.60 ± 0.01	0.54 ± 0.01	0.52 ± 0.01
5.00	1.00 ± 0.01	1.07 ± 0.01	1.11 ± 0.01	1.18 ± 0.03	1.23 ± 0.01
7.50	1.51 ± 0.01	1.62 ± 0.02	1.69 ± 0.02	1.79 ± 0.02	1.88 ± 0.03
10.0	1.80 ± 0.01	1.90 ± 0.03	2.03 ± 0.03	2.18 ± 0.02	2.30 ± 0.02
15.0	2.75 ± 0.01	2.98 ± 0.02	3.29 ± 0.03	3.45 ± 0.04	3.54 ± 0.02
		k'_2, s^{-1}			
2.50	4.6 ± 0.1	7.4 ± 0.2	15.7 ± 0.3	26.6 ± 0.9	52 ± 2
5.00	6.3 ± 0.1	10.1 ± 0.1	18.0 ± 0.3	33.3 ± 0.6	60 ± 1
7.50	8.3 ± 0.1	12.7 ± 0.2	21.5 ± 0.3	38.3 ± 0.6	65 ± 1
10.0	9.9 ± 0.1	14.6 ± 0.2	24.8 ± 0.3	42.2 ± 0.6	69 ± 2
15.0	12.9 ± 0.2	18.9 ± 0.2	30.2 ± 0.4	50.9 ± 0.9	81 ± 2

[a] Reaction Conditions: 0.10 mM ODI, 0.10 mM DPA and 5.0 mM ImH.

Table 2. Variation of k'_1 with H_2O_2 Concentration as a Function of Temperature in the Uncatalyzed Reaction of ODI with an Excess of H_2O_2[a]

$[H_2O_2]$, mM	**7.1,** °C	15.1, °C	24.9, °C	35.3, °C	45.1, °C
		k'_1, 10^{-2} s^{-1}			
2.50	1.52 ± 0.06	1.60 ± 0.06	1.81 ± 0.04	2.91 ± 0.09	2.55 ± 0.06
5.00	3.3 ± 0.1	3.4 ± 0.1	2.81 ± 0.09	3.8 ± 0.1	4.2 ± 0.1
7.50	5.1 ± 0.2	5.1 ± 0.2	4.5 ± 0.2	5.6 ± 0.2	6.6 ± 0.2
15.0	8.0 ± 0.2	11.1 ± 0.2	9.1 ± 0.3	11.7 ± 0.4	13.4 ± 0.3

[a] Reaction Conditions: 0.10 mM ODI, 0.10 mM DPA.

Table 3. Resolved Zero- and First-Order Contributions to k'_2 Obtained with 5.0 mM ImH and Second-Order Rate Constants for k_1 Obtained with and without 5.0 mM ImH, as a Function of Temperature

T, °C	5.0 mM ImH k_{2a}, s^{-1}	5.0 mM ImH k_{2b}, M^{-1} s^{-1}	5.0 mM ImH k_1, M^{-1} s^{-1}	no ImH k_1, M^{-1} s^{-1}
7.1	3.1 ± 0.1	670 ± 20	175 ± 5	5.1 ± 0.3
15.1	5.4 ± 0.3	910 ± 25	196 ± 5	7.6 ± 0.3
24.9	13 ± 1	1200 ± 100	212 ± 8	6.0 ± 0.4
35.3	23 ± 2	1900 ± 100	230 ± 10	7.3 ± 0.3
45.1	47 ± 4	2200 ± 120	240 ± 10	8.8 ± 0.5

tions in the range 2.5−15 mM are given in Figure 1, and the derived rate constants for the temperature range 7.1−45.1 °C are summarized in Table 1. The rate constants were determined using a large excess of H_2O_2 (2.5−15.0 mM) over ODI (0.10 mM) in the presence of 5.0 mM imidazole. As seen in Figure 1, the maximum signal increases with increasing H_2O_2 concentration.

The pseudo-first-order rate constant k'_1 increases linearly with increasing H_2O_2 concentration. Within experimental error, plots of k'_1 versus $[H_2O_2]$ pass through the origin; thus, the slope of each line was used to evaluate the corresponding second-order rate constant, which is 212 ± 8 M^{-1} s^{-1} at 25 °C. Values for the second-order rate constant at other temperatures are provided in Table 3. The second-order rate constant is only weakly dependent on temperature, increasing by only 40% between 7.1 and 45.1 °C. An Arrhenius plot gives an observed activation energy of 6.3 ± 0.6 kJ/mol for k'_1.

The pseudo-first-order rate constant, k'_2, increases linearly with increasing H_2O_2 concentration, as shown in Figure 2, but the plot of k'_2 versus $[H_2O_2]$ at each temperature has a large intercept. Both the slope and intercept increase with increasing temperature. The plots in Figure 2 were fit by linear regression to resolve the zero- and first-order contributions in $[H_2O_2]$ to the observed rate constant according to the equation:

$$k'_2 = k_{2a} + k_{2b}[H_2O_2] \qquad (3)$$

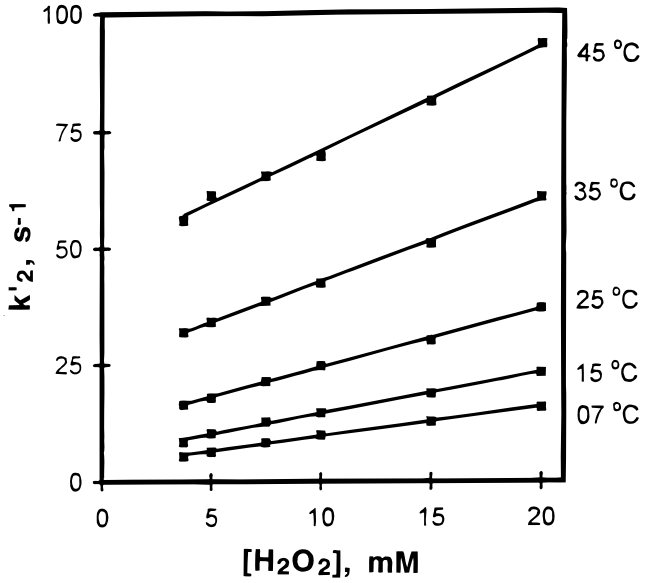

Figure 2. Pseudo-first-order fall rate constant, k'_2, as a function of hydrogen peroxide concentration using a large excess of H_2O_2 and imidazole catalysis. Conditions: 5.0 mM imidazole, 0.10 mM ODI, and 0.10 mM DPA.

The *y*-intercept, coefficient k_{2a}, represents a first-order reaction that is zero-order in concentration of hydrogen peroxide. The slopes of the plots in Figure 2 are the second-order rate constants, k_{2b}, for the reaction first-order in H_2O_2. These coefficients are summarized in Table 3. Although both k_{2a} and k_{2b} increase with increasing temperature, the reaction zero-order in H_2O_2 has the strongest effect on the reaction kinetics, increasing 14-fold between 7.1 and 45.1 °C. The first-order reaction in H_2O_2 increases only 5-fold in the same temperature range. Observed activation energies were calculated from Arrhenius plots of the resolved coefficients given in Table 3. The activation energy associated with the process zero-order in H_2O_2 is 52 ± 2 kJ/mol and that for the reaction first-order in H_2O_2 is 24 ± 2 kJ/mol.

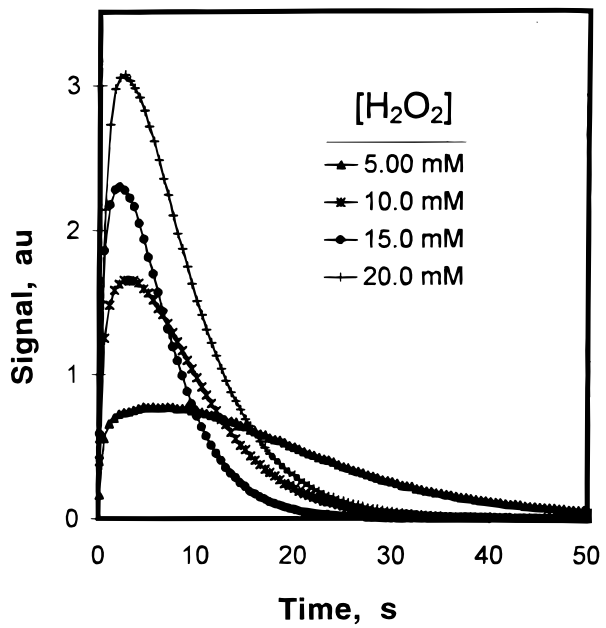

Figure 3. Chemiluminescence intensity versus time profiles obtained as a function of the H_2O_2 concentration in the uncatalyzed reaction of ODI and H_2O_2. Conditions: 0.10 mM ODI and 0.10 mM DPA.

Effect of Temperature and Hydrogen Peroxide Concentration on the Uncatalyzed Reaction of ODI with an Excess of H_2O_2. Chemiluminescence profiles obtained without imidazole and with H_2O_2 in large excess over ODI are illustrated in Figure 3. The profiles show a trend of increasing signal and reaction rate with increasing H_2O_2 concentration similar to the observations with imidazole present, Figure 1. Without imidazole, however, the rise in the CL signal contains at least two exponential components. Therefore, the uncatalyzed reaction does not follow the model for simple rise−fall kinetics. Rate constants, interpreted as k'_1, were estimated by fitting the fall portion of the curve to a single exponential. Values for k'_1 at different temperatures and hydrogen peroxide concentration are listed in Table 2.

The magnitude of k'_1 increases linearly with increasing H_2O_2 concentration, and within experimental error plots of k'_1 vs $[H_2O_2]$ pass through the origin. The calculated second-order rate constant at 25 °C is 6.0 ± 0.4 M^{-1} s^{-1}, which is 35 times less than the value of k'_1 obtained in the reaction catalyzed with 5.0 mM imidazole. The values for the second-order rate constant derived from k'_1 are given in Table 3 for the temperature range 7.1−45.1 °C. An Arrhenius plot provides an activation energy of 10.5 $\pm$ 1.7 kJ mol^{-1}, with the outlying point for $T = 15.1$ °C removed, for the uncatalyzed reaction.

Comparison of Profile Areas in the Catalyzed and Uncatalyzed Reaction of ODI with an Excess of Hydrogen Peroxide. The profile areas of the curves shown in Figures 1 and 3 were calculated in order to compare the effect of imidazole and hydrogen peroxide on the chemiluminescence quantum yield. Values for the profile area are summarized in Table 4. In the presence of imidazole, the area decreases by a factor of 1.8 as the H_2O_2 concentration is increased from 2.5 to 15.0 mM at 24.9 °C. The decrease in the profile area with increasing hydrogen peroxide concentration is approximately equal to the factor of 1.9 increase in k'_2 over the same concentration range, as seen in Table 1. Furthermore, a plot of profile area versus the ratio of k_{2a}/k'_2 shows that the zero-order process in $[H_2O_2]$ is the dominant light-producing pathway. The chemiluminescence profile areas obtained without imidazole remain essentially constant with increasing H_2O_2 concentration (Table 4) and are more than 1 order of magnitude greater than the areas from the imidazole-catalyzed reaction.

Table 4. Effect of Excess Hydrogen Peroxide Concentration on the Chemiluminescence Profile Area Obtained with and without 5.00 mM Imidazole at 24.9 °C[a]

$[H_2O_2]$, mM	no imidazole area, au	5.0 mM imidazole area, au
2.50	2100	150
5.00	2500	123
7.50	2300	101
10.0	2500	105
15.0	2400	84

[a] Reaction conditions: 0.10 mM ODI, 0.10 mM DPA.

Table 5. Effect of the Imidazole Concentration on k'_1, k'_2, and Profile Area Using Excess H_2O_2[a]

[ImH], mM	k'_1, s^{-1}	k'_2, s^{-1}	area, au
2.50	0.516 ± 0.006	12.2 ± 0.6	270
5.00	1.18 ± 0.01	15.2 ± 0.4	150
7.50	1.79 ± 0.01	15.5 ± 0.3	110
10.0	2.46 ± 0.03	15.6 ± 0.2	81
15.0	4.04 ± 0.03	15.3 ± 0.2	50

[a] Reaction conditions: 0.10 mM ODI, 0.10 mM DPA, 5.0 mM H_2O_2.

Variation of Imidazole Concentration Using Excess H_2O_2. The effects of imidazole concentration on k'_1, k'_2, and the profile area are summarized in Table 5. The rate constants were determined with imidazole concentrations ranging from 2.5 to 15.0 mM using constant H_2O_2 (5.0 mM) in excess over ODI (0.10 mM). Plots of the k'_1 and k'_2 versus imidazole concentration are shown in Figure 4. The pseudo-first-order rate constant k'_1 increases linearly with [ImH], and the derived second-order rate constant is 270 $\pm$ 12 M^{-1} s^{-1}. Increasing the imidazole concentration from 2.5 to 5.0 mM results in a slight increase in k'_2 from 12.2 to 15.2 s^{-1}. Beyond 5.0 mM imidazole, k'_2 is independent of the imidazole concentration. A 6-fold increase in the imidazole concentration results in a a factor of 5.4 decrease in the quantum yield of the reaction.

Variation of the ODI Concentration Using Excess Hydrogen Peroxide. The ODI concentration was varied from 0.10 to 0.40 mM in the reaction with an excess of hydrogen peroxide (15.0 mM) and imidazole (15.0 mM). The resulting rate constants and profile areas are given in Table 6. Both k'_1 and k'_2 increase by only 8% and 10%, respectively, for a 4-fold increase in ODI concentration, confirming that the reaction is pseudo first order in ODI to a good approximation when H_2O_2 is in large excess and that under these conditions there is very little back reaction of intermediate **B** with ODI or with an intermediate derived from ODI. A small increase in rate with increasing ODI concentration is expected since the catalyst ImH is produced in the reaction; also being a base, ODI may catalyze its own reaction. The profile area increases by a factor of 1.7 over the 4-fold increase in ODI concentration, much less than the expected factor of 4. As discussed below, ImH and the general bases lutidine and collidine greatly reduce the quantum yield

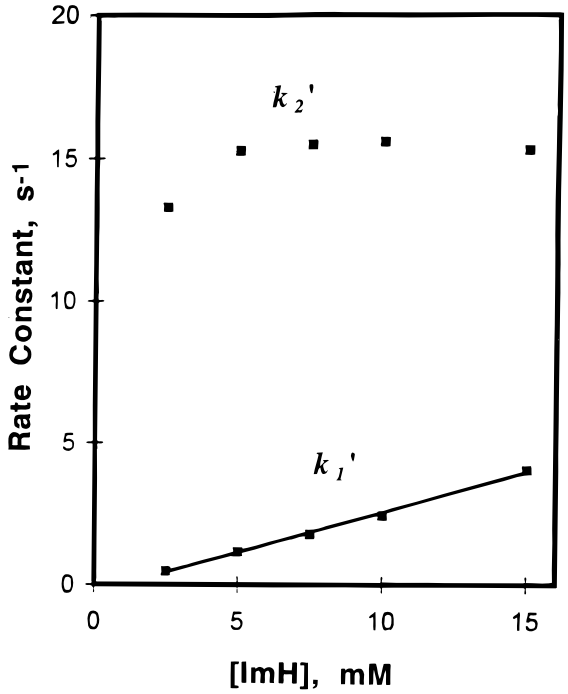

Figure 4. Pseudo-first-order rise and fall rate constants as a function of the imidazole concentration. Conditions: 0.10 mM ODI, 0.10 mM DPA, and 5.0 mM H_2O_2.

Table 6. Effect of the ODI Concentration on the Rise and Fall Rate Constant and Profile Area Using Excess H_2O_2 and 15 mM Imidazole[a]

[ODI], mM	k'_1, s^{-1}	k'_2, s^{-1}	area, au
0.10	8.00 ± 0.06	27.3 ± 0.3	33
0.15	7.92 ± 0.06	27.5 ± 0.1	40
0.20	8.77 ± 0.06	29.2 ± 0.2	41
0.25	8.14 ± 0.05	29.2 ± 0.1	58
0.30	8.39 ± 0.06	30.7 ± 0.3	49
0.35	8.37 ± 0.05	31.3 ± 0.3	56
0.40	8.64 ± 0.02	30.1 ± 0.4	56

[a] Reaction conditions: 15.0 mM H_2O_2, 15.0 mM imidazole, and 0.10 mM DPA.

of the reaction. Therefore, it is not surprising that ODI itself reduces the quantum yield.

Variation of ODI and Imidazole Concentrations Using Excess ODI Reaction Conditions. The chemiluminescence reaction was evaluated using a large excess of ODI (0.10−0.80 mM) over the hydrogen peroxide concentration (5.0 μM) in order to obtain additional insight into the mechanism. The reaction of 5.0 μM H_2O_2 in the presence of imidazole (5.0 mM) proceeds by a rapid signal increase, followed by a slow decay, as illustrated in Figure 5. The fast rise in chemiluminescence signal is characterized by a rate constant ranging from 12 to 24 s^{-1} and is 2−3 orders of magnitude faster than that describing the signal decline. The fast rise in signal required the use of a relatively low excess ODI concentration (0.10−0.80 mM) in comparison to the excess H_2O_2 concentrations discussed above (2.5−15 mM). This, in turn, required very low H_2O_2 concentrations of 5 μM in order to maintain pseudo-first-order conditions. The quantum yield is much higher, by more than an order of magnitude, than for conditions of excess H_2O_2, making the rate measurements possible at these low concentrations.

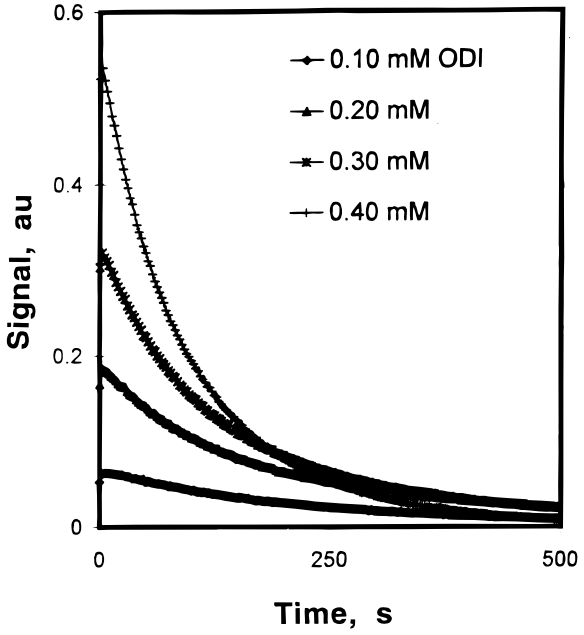

Figure 5. Chemiluminescence intensity versus time profiles obtained as a function of ODI using excess ODI. Conditions: 5.0 μM H_2O_2, 0.10 mM DPA, and 5.0 mM ImH.

Table 7. Effect of ODI Concentration on k'_1, k'_2, and Profile Area under Conditions of Excess ODI and 5.0 mM Imidazole[a]

[ODI], mM	k'_1, 10^{-2} s^{-1}	k'_2, s^{-1}	area, au
0.10	0.536 ± 0.005	23.8 ± 0.5	7.0
0.20	1.62 ± 0.04	15.6 ± 0.4	17
0.30	2.90 ± 0.08	13.5 ± 0.5	24
0.40	5.09 ± 0.06	13.0 ± 0.6	28
0.50	6.85 ± 0.07	12.2 ± 0.5	32
0.60	9.15 ± 0.05	12.2 ± 0.5	41
0.70	10.9 ± 0.1	12.4 ± 0.4	48
0.80	13.2 ± 0.3	12.5 ± 0.4	60

[a] Reaction conditions: 5.0 μM H_2O_2, 5.0 mM imidazole, 0.10 mM DPA.

Values for k'_1, k'_2, and the profile area are summarized in Table 7 as a function of excess ODI concentration. Again, we have taken the slower reaction to correspond to k'_1 and the faster reaction as k'_2, as justified by agreement of the second-order rate constants for the process **A** → **B**. A plot of k'_1 versus ODI concentration for an ImH concentration of 5.0 mM, Figure 6, is supralinear at low concentrations of ODI, but highly linear at high concentrations. Linear regression to the four data points at the highest ODI concentration (≥0.5 mM) yields a second-order rate constant of 208 ± 8 M^{-1} s^{-1}. This is in excellent agreement with the value of 212 ± 8 M^{-1} s^{-1} given above for the **A** → **B** reaction obtained with H_2O_2 in large excess. The cause of the nonlinear behavior at low concentrations is discussed below.

The variation of k'_2 with excess ODI concentration, as seen in Figure 7, is peculiar. The value of k'_2 decreases with increasing ODI concentration and levels off at ODI concentrations above 0.4 mM at a value of approximately 12 s^{-1}. The profile area and therefore the relative quantum yield increases with increasing ODI concentration, as seen in Figure 8, with a near-zero intercept. An explanation consistent with this behavior is given below.

Rate of Hydrogen Peroxide Decomposition in the Presence of Imidazole and DPA. A chemilumines-

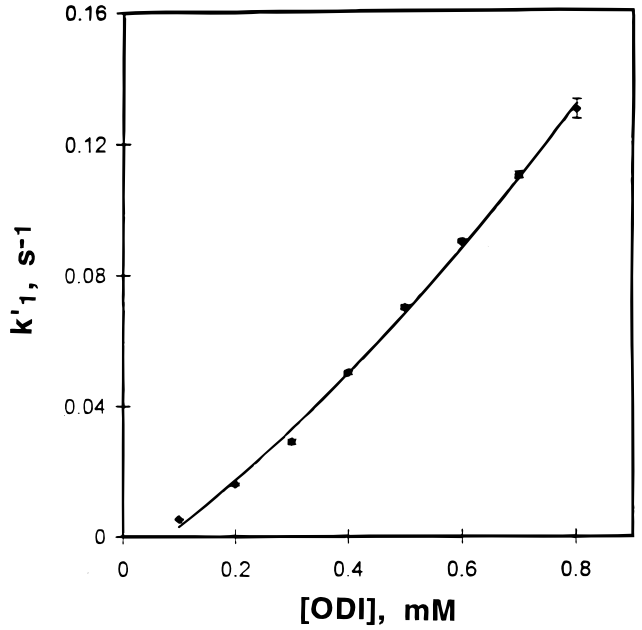

Figure 6. Effect of ODI concentration on k'_1 using excess ODI. Conditions: 5.0 μM H_2O_2, 5.0 mM ImH, and 0.10 mM DPA.

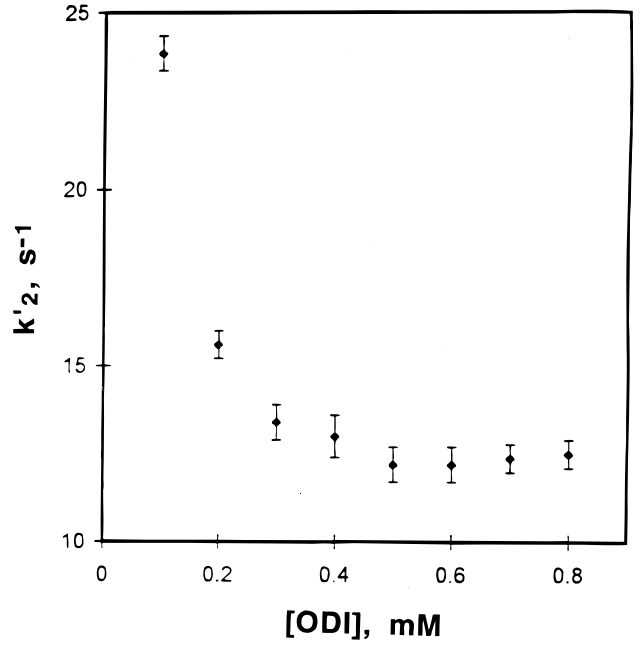

Figure 7. Effect of ODI concentration on k'_2 using excess ODI. Conditions: 5 μM H_2O_2, 5 mM ImH, and 0.10 mM DPA.

cence assay for H_2O_2 was performed under two conditions in an effort to characterize the possible loss of hydrogen peroxide by means other than by reaction with ODI. In the first experiment, 10.0 mM H_2O_2 and 20.0 mM ImH were premixed for varying lengths of time and subsequently analyzed by reaction with 0.80 mM ODI premixed with 0.20 mM DPA. Measurements were made by 1:1 mixing of the two solutions in the stopped-flow reactor for 200 and 500 s intervals over a period of 1 h. To determine whether DPA contributed to the decay of the hydrogen peroxide concentration, a second experiment was performed in which the same concentrations of H_2O_2, ImH, and DPA were premixed and chemiluminescence measurements made at the same intervals. The maximum chemiluminescence signal obtained for premixing

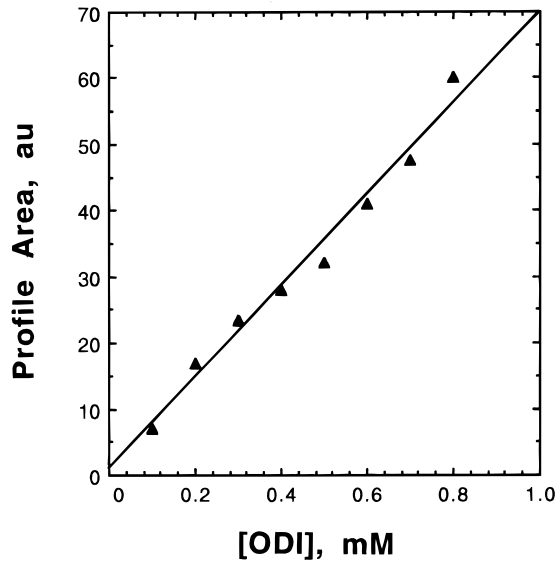

Figure 8. Effect of ODI concentration on the profile area with H_2O_2 as the limiting reagent. Conditions: 5.0 μM H_2O_2, 5.0 mM ImH, and 0.10 mM DPA.

H_2O_2 and ImH decreased with a first-order rate constant of 2.2×10^{-4} s^{-1}. The signal obtained with H_2O_2 premixed with both ImH and DPA decayed with a rate constant of 3.2×10^{-4} s^{-1}. These apparent rate constants are more than an order of magnitude smaller than those measured for k'_1 with ODI in large excess, while the imidazole concentration was four times larger than in a typical experiment.

Comparison of the General Base Catalysts Lutidine and Collidine with Imidazole. To clarify the catalytic role of imidazole, the reaction was studied using two sterically hindered bases, lutidine and collidine:

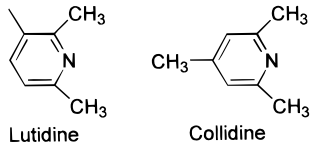

(4)

Lutidine ($pK_a = 6.5$) and collidine ($pK_a = 7.2$) have base strengths similar to imidazole ($pK_a = 6.95$) but are sterically hindered, nonproton-donating bases. The chemiluminescence profiles obtained using lutidine, collidine, and imidazole are compared with the noncatalyzed profile in Figure 9. The rate constants obtained using 5.0 mM amine base, 5.0 mM H_2O_2, and 0.10 mM ODI are compared in Table 9. The rate constants for lutidine and collidine show an increase with increasing aqueous pK_a. However, in the presence of imidazole, k'_1 and k'_2 are twice those obtained using collidine. The catalytic effect of imidazole on the reaction of ODI with H_2O_2 apparently exceeds predictions based solely on aqueous pK_a. Another significant observation, apparent in Table 9, is that all three bases cause very large decreases in the quantum yield. Imidazole, however, enhances the reaction rate with considerably less loss of quantum yield than the general bases lutidine and collidine.

Proposed Mechanism. The reaction of 1,1′-oxalyldiimidazole with hydrogen peroxide in the presence of a fluorophore generates chemiluminescence with a complex dependence on each of the reagents, ODI, H_2O_2, and the

Scheme 1

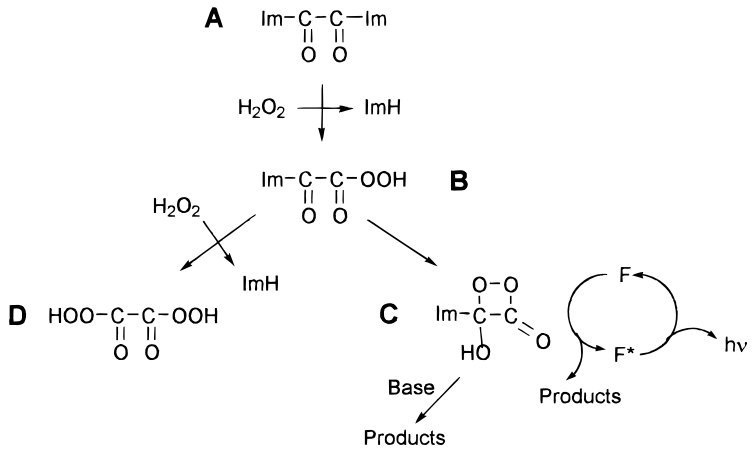

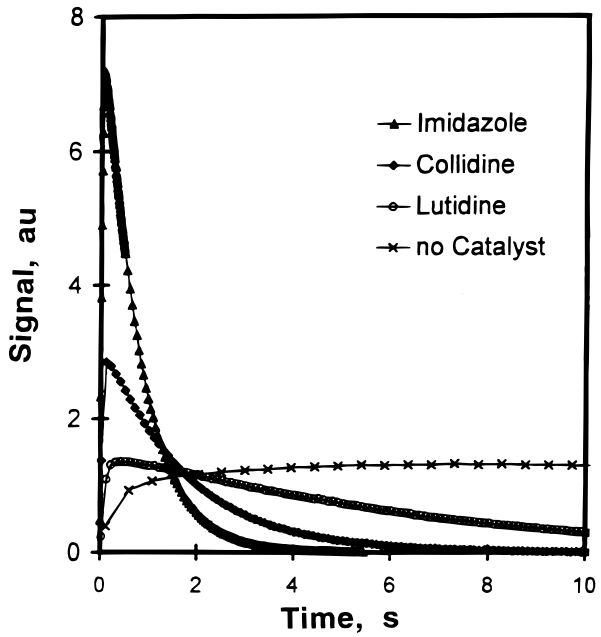

Figure 9. Chemiluminescence profiles obtained with imidazole, collidine, and lutidine and the profile obtained in the absence of a catalyst. Conditions: 5.0 mM catalyst, 0.10 mM ODI, 5.0 mM H_2O_2, temperature of 45 °C.

Table 8. Effect of Imidazole Concentration on k'_1 and Profile Area with Excess ODI[a]

[ImH], mM	k'_1, $10^{-2}s^{-1}$	area, au
2.50	0.516 ± 0.006	15
5.00	1.18 ± 0.01	15
7.50	1.79 ± 0.01	9.0
10.0	2.46 ± 0.03	6.0
15.0	4.04 ± 0.03	4.0

[a] Reaction conditions: 0.20 mM ODI, 0.10 mM DPA, 5.0 μM H_2O_2.

catalyst imidazole. By studying the reaction under pseudo-first-order conditions with ImH and either H_2O_2 or ODI in large excess over the remaining limiting reagent, it is possible to define two clearly different light-generating pathways. Mechanisms consistent with all of the results obtained are provided as Scheme 1 for H_2O_2 in large excess and Scheme 2 for ODI in large excess.

Mechanism for Excess H_2O_2 Conditions. Under conditions of a large excess of H_2O_2 over ODI, both k'_1 and k'_2 increase linearly, and the quantum yield decreases with increasing H_2O_2 concentration. In our proposed mechanism given by Scheme 1, nucleophilic substitution of H_2O_2 for imidazole in ODI results in an imidazoyl peracid, **B**, analogous to the first reaction step proposed for peroxyoxalate chemiluminescence:[1–5]

Table 9. Effect of Catalysts on the Rise and Fall Rate Constants Using a Large Excess of H_2O_2 over the ODI Concentration[a]

catalyst	pK_a	k'_1, s^{-1}	k'_2, s^{-1}	area, au
none		0.042 ± 0.001	0.42 ± 0.03	2700
lutidine	6.5	0.217 ± 0.002	8.6 ± 0.3	60
imidazole	6.95	1.23 ± 0.01	60.2 ± 0.8	380
collidine	7.2	0.45 ± 0.02	27 ± 3	10

[a] Conditions: 0.10 mM ODI, 5.0 mM H_2O_2, 5.0 mM catalyst, temperature of 45 °C.

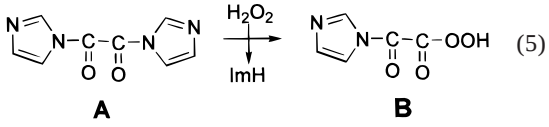

(5)

This reaction results in the observed first-order dependence of k'_1 on H_2O_2 concentration. The reaction would be expected to be base catalyzed, giving rise to the first-order dependence of k'_1 on imidazole concentration. The direct formation of an intermediate leading to chemiluminescence results from the intramolecular cyclization of the imidazoyl peracid to form an imidazoyl-hydroxydioxatanone, species **C**.

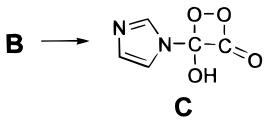

(6)

This cyclic peroxide is similar to other proposals made for the structure of the high-energy intermediate.[3,4] Dioxatanones[14,15] similar to **C** have been shown to produce the singlet excited state of highly fluorescent acceptor molecules in a chemically initiated electron exchange luminescence (CIEEL) reaction.[16]

The first-order dependence of k'_2 on H_2O_2 is best explained by a second substitution of H_2O_2 for imidazole

(14) Adam, W.; Liu, J. *J. Am Chem. Soc.* **1972**, *94*, 2894–2895.
(15) McCapra, F. *Prog. Org. Chem.* **1973**, *8*, 231.
(16) Schuster, G. B. *Acc. Chem. Res.* **1979**, *12*, 366–373.

Scheme 2

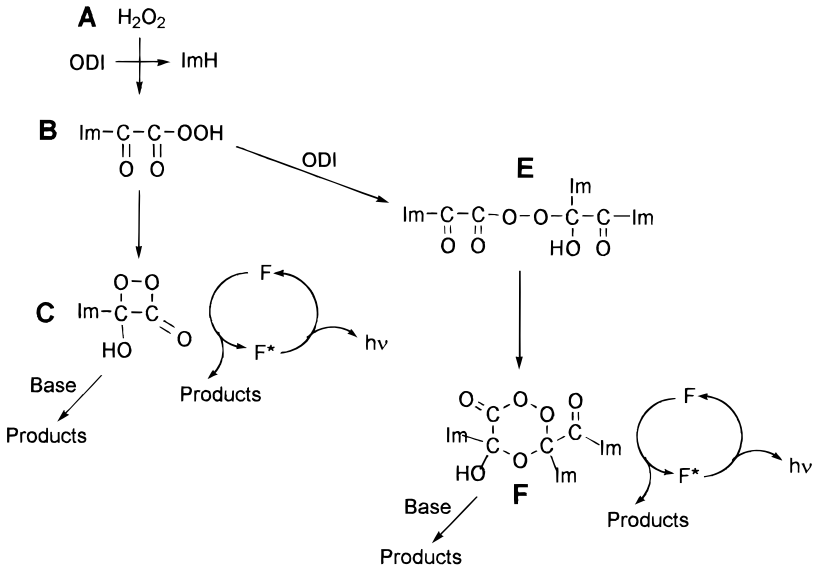

to form the dihydroperoxyoxalate, species **D**:

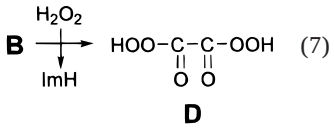

(7)

The decrease in quantum yield with increasing H_2O_2 concentration indicates that species **D** does not lead to significant chemiluminescence via an analogous cyclization.

As would be expected, cyclization of species **B** has a relatively high activation energy of 52 kJ/mol. It is difficult to explain, however, why the second substitution of H_2O_2 would have a much faster rate constant than the first substitution (1350 M^{-1} s^{-1} vs 212 M^{-1} s^{-1}) while displaying a much higher activation energy (24 vs 6.3 kJ/mol). This could possibly be explained by the additional observation that the first substitution is imidazole-catalyzed, while the second substitution is not. Apparently, imidazole reduces the activation energy for the first substitution while making the transition state less favored entropically, perhaps through steric hindrance. The unique nature of imidazole catalysis is discussed below.

Mechanism for Excess ODI Conditions. The mechanism of the reaction with ODI in large excess over H_2O_2 has some unusual features. A plot of the pseudo-first-order rate constant k'_1 vs [ODI] is supralinear at low concentrations but highly linear at concentrations at or above 0.4 mM (Figure 6). The rate constant k'_2 actually decreases with increasing ODI concentration at the lowest concentrations and then levels off to a constant value (Figure 7). At the same time, the quantum yield increases with increasing ODI concentration (Figure 8). Furthermore, the overall quantum efficiency is more than an order of magnitude greater with ODI in large excess (actual value depends on the ODI concentration) than when H_2O_2 is in large excess. The mechanism given in Scheme 2 provides an explanation of all of the above results for conditions of excess ODI concentration. In this scheme, intermediate **B** may either cyclize and produce relatively weak chemiluminescence, as in Scheme 1 for excess H_2O_2, or react with another molecule of ODI to form the peroxide **E**:

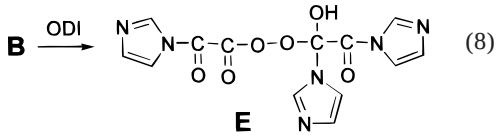

(8)

The formation of **E** and its subsequent reactions are analogous to the earlier proposal of Milofsky and Birks[5] for the photoinitiated peroxyoxalate reaction. In that work small quantities of H_2O_2 were formed in the presence of a large excess of oxalate ester by means of a photochemical reaction. Again, analogous to the peroxyoxalate reaction,[5] we propose that **E** may cyclize to form the high-energy intermediate **F**:

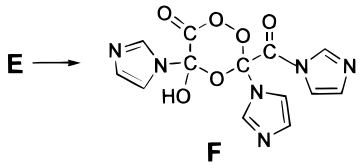

(9)

The decrease and leveling off of k'_2 with increasing ODI concentration (Figure 7) may be explained by a shunting of the reaction pathway to intermediates **E** and **F** due to reaction of **B** with ODI. In this case, the pseudo-first-order rate constant k'_2 would decrease with increasing [ODI] and level off at the value of the first-order rate constant for cyclization of **E**. Since the lifetime of **B** is short compared to the time constant for conversion of **A** to **B**, species **B** quickly reaches steady state. If we apply the steady-state approximation to **B** and treat the formation of **E** as the pseudo-first-order rate constant k'_1, we have:

$$k'_1 = k_{A\rightarrow B}k_{B\rightarrow E}[ODI]^2/(k_{B\rightarrow C} + k_{B\rightarrow E}[ODI]) \quad (10)$$

Note that in the limit of low ODI concentration a plot of k'_1 versus [ODI] is quadratic in [ODI], while in the limit

of high ODI concentrations k'_1 is given by

$$k'_1 = k_{A\rightarrow B}[\mathrm{ODI}] \qquad (11)$$

Thus, at higher ODI concentrations, the second-order rate constant $k_{A\rightarrow B}$ should be the same as that obtained with H_2O_2 in large excess, which is in agreement with the observations. The increasing rate of path **B** → **E** relative to path **B** → **C** with increasing [ODI] qualitatively explains (1) the increase in quantum yield with increasing ODI concentration, (2) the quadratic dependence of k'_1 on [ODI] at low concentrations and linear dependence at high [ODI], and (3) the decrease and leveling off of k'_2 with increasing [ODI]. This mechanism appears to require that the cyclization reaction **B** → **C** be two to three times faster (~25−35 s^{-1} vs 13 s^{-1} for 5 mM ImH) in the presence of excess ODI than in the presence of excess H_2O_2, although such quantitative conclusions based on a simplified rise−fall kinetics analysis of a mechanism that is obviously more complicated may not be valid. In any case, the absence of high concentrations of the weak acid H_2O_2 might facilitate a more rapid cyclization, and ODI, which is dibasic, could also accelerate the cyclization.

The high-energy, cyclic intermediate **F** may transfer energy to a fluorophore via the CIEEL mechanism, decomposing to form one molecule of CO_2, one molecule of ImCOOH (which might simultaneously decompose to form CO_2 and ImH) and one molecule of ODI. These are the same decomposition products of high-energy intermediate **C** plus the additional product ODI. Previous kinetics work has shown that the charge-transfer steps leading to chemiluminescence are fast relative to the formation of an initial intermediate.[2−6] The rate constants obtained for the reaction of ODI and H_2O_2 were unaffected by variations in the DPA concentration, confirming that the final reactions leading to chemiluminescence are kinetically unobservable.

Roles of Imidazole. Imidazole catalyzes the formation of the imidazoyl-peracid with a larger catalytic effect on the reaction than just "general-base" catalysis (Table 9). On the basis of previous observations of the ability of imidazole to serve as a proton source and sink in many catalyzed reactions,[17,1817,18] a concurrent general-base and general-acid catalytic role of imidazole involving two molecules of imidazole is possible. One molecule of imidazole could act as a base catalyst promoting the addition of hydrogen peroxide while another molecule of imidazole protonates one of the imidazoles of ODI to form an imidazolium ion, a much better leaving group. Such a mechanism, however, would be expected to show a second-order dependence on imidazole concentration, while only a first-order dependence is observed.

Another possibility is that addition of imidazole to one of the carbonyls enhances the rate of nucleophilic attack of H_2O_2 at the remaining carbonyl:

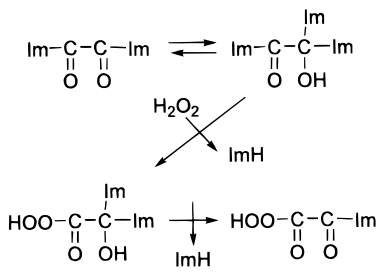

(12)

Such a mechanism could explain why the first substitution of H_2O_2 for ImH in ODI, which is ImH catalyzed, is relatively slow despite having a very low activation energy of only 6.3 ± 0.6 kJ/mol. The necessity of adding one molecule of ImH in order to lower the energy of the transition state could slow the reaction via steric hindrance, with the result that although the reaction is much faster than the uncatalyzed reaction it is much slower than expected based on comparison with similar reactions. The second substitution, for example, which is uncatalyzed by ImH, is much faster despite having an activation energy of 24 ± 2 kJ/mol.

For both reaction conditions, excess H_2O_2 or excess ODI, an increase in the imidazole concentration results in a large decrease in the chemiluminescence quantum yield (Tables 4, 5, and 8). Since the general base catalysts lutidine and collidine also have strong quenching effects on the quantum yield, it is possible that all three bases promote the unimolecular decomposition of the cyclic peroxide intermediates by deprotonation, as indicated in Schemes 1 and 2. Ironically, it may be that deprotonation of **C** to cause Im^- elimination and formation of 1,2-dioxetanedione, the long-postulated peroxyoxalate intermediate, may actually be the major factor in reducing the quantum yield of the reaction when H_2O_2 is in excess. General bases could cause the decomposition of the cyclic peroxide **F** by deprotonation as well.

Consistent with the results obtained here, several researchers have described either multiexponential profiles at low catalyst concentration or inconsistent results in the absence of a catalyst for the reaction of oxalate esters with H_2O_2.[2,6,19] The reaction appears to be even more complex in the absence of a catalyst.

Conclusions

The reaction of 1,1′-oxalyldiimidazole with hydrogen peroxide in the presence of imidazole follows two well-defined pathways to two different high-energy intermediates. The relative contributions of those pathways to the chemiluminescence signal can be varied by adjusting the concentrations of H_2O_2 and ODI. Structures of the intermediates are proposed based on the orders of reaction with respect to the reagents and on the assumption that a CIEEL mechanism is responsible for the energy-transfer step. The proposed mechanism is analogous to that proposed earlier for the peroxyoxalate reaction.[5] Imidazole is shown to be more effective than the general base catalysts lutidine and collidine, which have similar pK_a's. Nucleophilic catalysis, as proposed for imidazole in the peroxyoxalate reaction, is not applicable to ODI. A possible mechanism for this additional means of catalysis that is consistent with the observed activation energies is proposed.

JO9917487

(17) Bender, M. L.; Bergeron, R. J.; Komiyama, M. *The Bioorganic Chemistry of Enzyme Catalysis*; Wiley-Interscience: New York, NY, 1984; pp 45, 130.
(18) Seoud, O. A. E.; Menegheli, P.; Pires, P. A. R.; Kiyan, N. Z. *J. Phys. Org. Chem.* **1994**, *7*, 431−436.
(19) Alvarez, F. J.; Parekh, N. J.; Matuszewski, B.; Givens R. S.; Higuchi, T.; Schowen, R. L. *J. Am. Chem. Soc.* **1986**, *108*, 6435−6437.